

Calculated crystal-field parameters of SmCo_5

Manuel Richter*

Condensed Matter Theory Group, Institute of Physics, University of Uppsala, Box 530, S-75121 Uppsala, Sweden

Peter M. Oppeneer*

Institut für Festkörperphysik, Technische Hochschule Darmstadt, Hochschulstrasse 6, D-W-6100 Darmstadt, Germany

Helmut Eschrig*

Institut für Festkörperforschung, Institut für Festkörper- und Werkstofforschung Dresden e.V., D-O-8027 Dresden, Germany

Börje Johansson

Condensed Matter Theory Group, Institute of Physics, University of Uppsala, Box 530, S-75121 Uppsala, Sweden

(Received 5 June 1992)

From a first-principles density-functional (DF) calculation of the charge distribution all crystal-field (CF) parameters for the $4f$ states at the Sm site in SmCo_5 have been evaluated. The calculation is based on an optimized linear combination of atomic orbitals scheme for the conduction-electron magnetism and on an "open $4f$ core shell" treatment of the localized Sm $4f$ moments. Real-space integrations are used to evaluate both on-site and lattice contributions to the CF parameters. It is explicitly shown that there is no justification in neglecting either of these contributions. In comparison to available experimental values, DF calculations are found to yield the correct sign for all CF parameters, but to overestimate considerably the magnitude of the most essential second-order parameter, A_2^0 .

I. INTRODUCTION

Among the variety of binary and, more recently, ternary rare-earth-transition-metal (R - T) compounds which have been investigated for their hard magnetic properties during the last decades,^{1,2} SmCo_5 plays the role of a precursor. In spite of its rapid technological utilization on an industrial scale,³ the theoretical understanding of its intrinsic physical properties is largely incomplete. Only one of the three intrinsic properties relevant for an application as a permanent magnetic material has so far been satisfactorily explained from first principles: Early calculations of the saturated moment M_s of SmCo_5 and related compounds⁴ yielded reasonable values (for more recent results see Ref. 5). The other two properties important for its application, the Curie temperature (T_C) and the magnetocrystalline anisotropy energy (MAE), are more difficult to treat theoretically. We are not aware of any theoretical estimation of T_C for this specific compound, something which would most likely require the introduction of a model Hamiltonian. The MAE, on the other hand, is by definition the energy difference between the easy and hard axes of magnetization.⁶ Therefore, the MAE at zero temperature is a ground state property and should, at least in principle, be accessible to *ab initio* calculations.

In a more general way, the MAE can be introduced as a temperature (T) and direction (Θ) dependent free energy $F(T, \Theta)$.⁷ From a comparison with several isostructural compounds, Buschow *et al.*⁷ concluded that the MAE of

SmCo_5 is dominated by the Sm $4f$ part and that the itinerant $3d$ electrons contribute only by about one-third at $T = 0$ K. This itinerant contribution has been evaluated both by Nordström *et al.*⁸ and by Daalderop *et al.*⁹ for the isostructural YCo_5 ferromagnetic compound with encouraging results. As regards the localized $4f$ contribution, a description in terms of an ionic model Hamiltonian for the anisotropy seems justified.⁷ Besides the strength of the spin-orbit coupling, which is fairly well known, and that of the exchange field, crystal-field (CF) parameters enter this model. These CF parameters have been estimated semiempirically by fitting to experimental data.^{7,10-12}

CF parameters are demanding quantities to calculate in an *ab initio* treatment of the MAE. It was some ten years ago when Fulde stated the following:¹³ "Although the description of crystal fields is rather well known and standard by now, their computation from microscopic theory is far from being understood." Meanwhile, several attempts¹⁴⁻¹⁶ have been made to calculate CF parameters of rare-earth-transition-metal (R - T) compounds from a realistic charge distribution, i.e., beyond oversimplified point charge models (PCM). These attempts have either been based on non-self-consistent calculations¹⁴ or do not include lattice contributions to the crystal field.^{15,16} A first-principles calculation which is complete in this sense is due to Daalderop *et al.*^{9,17} That calculation, however, gives a result for the second-order CF parameter of Gd in GdCo_5 deviating from experimental values by a factor of 2-4. In the case of el-

emental Tb, Novák and Kuriplach³⁷ report a deviation by a factor of 2 between theoretical and experimental results.

In the following section, the consistency between the “open 4f core shell” concept for the electronic structure of *R-T* intermetallics^{18,5} and the commonly used semiempirical description of MAE in these compounds is shown. Subsequently, in Sec. III, recent first-principles calculations of CF parameters are briefly reviewed and compared with our approach. Our results are presented in Sec. IV. They are discussed and compared with experimental values and with theoretical results from Refs. 9 and 17. Conclusions are drawn in Sec. V.

II. THE MODEL

From a theoretical point of view, magnetic *R-T* compounds are of particular interest, since they contain both itinerant and localized magnetic subsystems. The 3d electrons show itinerant behavior and are well described within the local spin density approximation¹⁹ (LSDA) of density-functional theory. In contrast, the 4f electrons in *R-T* intermetallics, except some of those containing Ce, are localized due to the large intra-atomic correlation and do not contribute to the chemical bonding.²⁰ The rare-earth 5d electrons are parasitically spin polarized, and 3d-5d hybridization couples the two subsystems antiferromagnetically.²¹

Applying standard LSDA electronic structure theory to these compounds not only meets practical difficulties (bad convergence of the Kohn-Sham equations caused by the high *f* density of states near the Fermi level), but is also questionable since strong correlations may produce discontinuities in the derivatives of the Hohenberg-Kohn energy functional $E[\rho]$.²² Furthermore, the 4f bandwidth W is too high if intra-atomic correlations are neglected. A simple model beyond LSDA which is capable of overcoming these difficulties has recently been applied by some of the authors:^{18,5} the 4f shell is considered to remain in its ionic ground state configuration, but is subject to both Hartree and exchange (ex) interaction with the other electrons. Thus, 4f correlation is accounted for by cutting off all hybridization between the 4f states and the conduction states, corresponding to the limit $U_{\text{eff}}/W \rightarrow \infty$, where U_{eff} is the screened intra-atomic correlation energy. On the other hand, the effective spin-polarized potential is created by all electrons (4f included). Two restrictions will be introduced, which might limit the justification of calling the present calculations *ab initio*. However, both are rather obvious and straightforward by physical intuition. First, the number of 4f electrons is constrained to its trivalent atomic value and second, the 4f spin density is scaled to obtain the Russel-Saunders spin moment. It should be mentioned

that the latter restriction is much weaker than the former, since the size of the 4f moment turns out to have only minor influence on the valence electron polarization in *T*-rich *R-T* compounds.²³ Investigations by other authors utilizing the conceptual simplicity and suitability of this “open 4f core shell” treatment were recently performed and are in progress.¹⁶

The successful semiempirical treatment of 4f based MAE (Refs. 7, 10, 11, and 24) fits well with the above picture, providing strong evidence for its justification from the experimental side. This treatment starts from a model Hamiltonian determining the energy levels of the *R* 4f shell in its ionic configuration, but perturbed by the crystalline environment. This Hamiltonian includes spin-orbit (H_{SO}), *R-T* exchange (H_{ex}), and crystal-field (H_{CF}) interactions, the relative strengths of which can roughly be described as

$$H_{\text{SO}} : H_{\text{ex}} : H_{\text{CF}} \sim 10^4 \text{ K} : 10^3 \text{ K} : 10^2 \text{ K}$$

in most cases. As a consequence, the total angular momentum J of the 4f shell is a good quantum number and the nonspherical 4f charge density rotates rigidly together with the 3d magnetization (which determines the direction of H_{ex}) when an external field is applied. Then, considering the second part of the relation above, to first order the MAE equals the difference of the 4f JM ground state expectation values, $\langle JM | H_{\text{CF}} | JM \rangle$, between different axes of magnetization. Even in more involved cases, as for our present case of Sm, where two low-lying configurations with $J = \frac{5}{2}$ and $J = \frac{7}{2}$ compete, the description of the temperature dependent MAE is possible in terms of CF parameters by taking into account the mixing of the higher multiplets with the ionic ground state.⁷ Very recently, Ibarra *et al.*¹² employed the described model for the case of noncollinear arrangements of the *R* and *T* moments. This situation may arise if the easy direction of magnetization does not coincide with any of the crystallographic axes (easy cone).

Both the “open 4f core shell” treatment and the semiempirical description of the 4f contribution to the MAE are essentially equivalent, since they are based on the same idea: the 4f electrons are coupled to the other electrons via Hartree and exchange interactions, but do not hybridize. Consequently, the CF parameters obtained from our first-principles calculation should have the same meaning as those entering the model Hamiltonian for the evaluation of the MAE.

III. CALCULATION OF CF PARAMETERS

In general, the (Hartree) interaction energy of the 4f electrons with all other charges (nuclear charges included) can be written

$$E_{4f}^H = \iint d\mathbf{R} d\mathbf{r} \frac{\rho(\mathbf{R})\rho_{4f}(\mathbf{r})}{|\mathbf{R} - \mathbf{r}|} = \sum_{l=0}^6 \sum_{m=-l}^l \frac{4\pi}{2l+1} \iint d\mathbf{R} d\mathbf{r} \frac{r_{<}^l}{r_{>}^{l+1}} Z_{lm}(\mathbf{R}) Z_{lm}(\mathbf{r}) \rho(\mathbf{R}) \rho_{4f}(\mathbf{r}), \quad (1)$$

with $r_{<} = \min(r, R)$, $r_{>} = \max(r, R)$. Z_{lm} are real spherical harmonics (also called Tesseral harmonics; remark on the notation: several authors prefer Z_{lm}^c , Z_{lm}^s instead of the present $Z_{l|m|}$, $Z_{l-|m|}$). The restriction to a maximum

l value is possible since ρ_{4f} does not contain higher momenta than $l = 6$. The spherical term is left out (see the discussion below),

$$E_{4f}^{H,\text{nonspherical}} \equiv \langle H_{\text{CF}} \rangle,$$

and the angular dependent part of the $4f$ density is put into the Stevens coefficients Θ_l specific to the R ion:²⁵

$$H_{\text{CF}} = \sum_{l>0}^6 \sum_{m=-l}^l \Theta_l \langle r^l \rangle_{4f} O_l^m A_l^m, \quad (2)$$

where O_l^m denote Stevens operator equivalents²⁵ and

$$A_l^m = \frac{4\pi}{2l+1} \int d\mathbf{R} C_{lm} Z_{lm}(\mathbf{R}) \rho(\mathbf{R}) \int dr \frac{r^l}{r^{l+1}} r^2 \rho_{4f}(r) \bigg/ \int dr r^{l+2} \rho_{4f}(r) \quad (3)$$

are the crystal-field parameters as introduced for the case $(l, m) = (2, 0)$ by Coehoorn.¹⁵ The original formulation (see, e.g., Ref. 26) takes no account of the overlap between $4f$ and CF generating charges. Equation (3) yields CF parameters more appropriate for the description of $4f$ properties but not suitable for the interpretation of nuclear (e.g., Mössbauer) data.

Contributions of the exchange potential to A_l^m can be neglected, since these are produced by *local* deviations of the (non- $4f$) charge density from a spherical distribution, which are certainly very small in the region of the $4f$ shell (cf. Fig. 3 and the related discussion at the end of Sec. IV).

By symmetry, only A_2^0 , A_4^0 , A_6^0 , and A_6^6 are nonzero at the R site in the hexagonal CaCu₅ structure under consideration, and A_2^0 is generally assumed to have the main influence on the MAE (it essentially determines the sign of the anisotropy). The explicit expressions for C_{lm} and Z_{lm} are

$$\begin{aligned} C_{20} &= \sqrt{\frac{5}{16\pi}}, & C_{40} &= \sqrt{\frac{9}{256\pi}}, \\ C_{60} &= \sqrt{\frac{13}{1024\pi}}, & C_{66} &= \sqrt{\frac{6006}{4096\pi}}, \\ Z_{20} &= C_{20}(3z^2 - r^2)/r^2, \\ Z_{40} &= C_{40}(35z^4 - 30z^2r^2 + 3r^4)/r^4, \\ Z_{60} &= C_{60}(231z^6 - 315z^4r^2 + 105z^2r^4 - 5r^6)/r^6, \\ Z_{66} &= C_{66}(x^6 - 15x^4y^2 + 15x^2y^4 - y^6)/r^6. \end{aligned}$$

At this point, some remarks on the validity of the commonly used approach for the determination of CF parameters from experimental MAE data^{7,10-12} seem to be appropriate. By comparing data for isostructural compounds containing different rare-earth elements, the $4f$ contribution to the MAE can be well estimated. A model Hamiltonian is constructed including spin-orbit, exchange, and crystal-field interactions and diagonalized either using the lowest or additionally excited multiplets. Usually, one parameter for the exchange field and one or several CF parameters are used to fit the temperature dependence of the MAE. There are two essential approximations employed in this scheme: (i) the independence of the CF parameters on temperature and (ii) the independence of these parameters on the direction of magnetization. The first approximation is certainly

justified, since the bandwidth is at least 1 order of magnitude larger than T_C . As concerns the second, we note that the valence charge density depends on the direction of magnetization via spin-orbit coupling. This might not only influence the nonspherical CF, but also introduce a dependence of the *spherical* part of Eq. (1) on the direction of magnetization. The size of this effect has yet to be investigated by means of fully relativistic calculations. Nonetheless we assume the current approximation to be valid, since the relative strength of CF and spin-orbit interaction is just the opposite for the T $3d$ electrons than for the R $4f$ electrons.

We now turn to the estimation of A_l^m from a *calculated* charge distribution. Two points have to be observed in evaluating the CF parameters according to Eq. (3). At first, an accurate charge density is needed: LSDA calculations are known to yield accurate charge distributions even in strongly correlated systems. Then the related integrations have to be done, where convergence with respect to the individual density contributions has to be observed. This is considerably facilitated when the basis of the charge density representation is well adapted to the physical problem at hand.

In the following, we briefly address the several approaches that were previously undertaken to compute the A_l^m .

Early approaches to this task, see, e.g., Ref. 27, employed a point-charge model, i.e., the CF generated by a lattice of ionic point charges was calculated. Then the influence of conduction electrons was included by more or less empirical shielding (or, antishielding) factors. Consequently, the set of crystal-field parameters was replaced by another semiempirical set of point charges and shielding factors. Nevertheless, rather impressive results have been obtained by applying the same set of semiempirical effective point charges to different compounds.²⁸

Recently, Coehoorn¹⁵ pointed out the importance of so-called on-site contributions to the crystal field in R intermetallics, i.e., contributions generated by the nonspherical valence charge density belonging to the R atom under consideration. He calculated A_2^0 (on site) for Gd in Gd₂Fe₁₄B and for Gd impurities in Y with the augmented spherical wave (ASW) scheme.²⁹ The result was about 25% higher than the experimental values for isostructural compounds, which might be attributed to the complete neglect of lattice contributions. Point-charge es-

timates of $A_2^0(\text{lattice})$ were, in contrast to the on-site terms, dependent on the choice of atomic sphere radii employed in the ASW. The astonishing fact that the total value $A_2^0(\text{on site}) + A_2^0(\text{lattice})$ depends on the sphere radii points to the necessity of going beyond the PCM for the lattice part.

Subsequently similar calculations were reported by Hummler and Fähnle¹⁶ within the LMTO formalism. These authors investigated $R_2\text{Fe}_{14}\text{B}$ for R elements different from Gd, using the “open $4f$ core shell” treatment discussed above. The results for $A_2^0(\text{on site})$ depend on the sphere radii and are larger than related experimental values by 30–60%. Another calculation for the same type of compounds is due to Zhong and Ching,¹⁴ based on a non-self-consistent LCAO calculation. Despite being comparable with experimental data, their results cannot be regarded as reliable, since every effect of charge redistribution when forming an intermetallic compound from its constituents is neglected. It is true that metallic screening prevents large charge transfers, but the CF is very sensitive to even tiny changes in the electronic charge distribution.

Up to now the only published first-principles calculation of CF parameters for an RT_5 compound has been carried out by Daalderop *et al.*^{9,17} in the full-potential linearized augmented plane wave (FLAPW) scheme.³⁰ These authors utilize the Tesseral harmonics expansion of the crystal potential used in FLAPW and calculate A_7^m for GdCo_5 . This approach should in principle be complete with respect to accounting both for the on-site and lattice contributions, but leads to a value of A_2^0 much larger than the experimental results.

In the following, our present method will be outlined in some detail. The calculations reported below are done using the optimized linear combination of atomic orbitals (LCAO) method³¹ in a scalar relativistic version.³² The general advantages inherent to standard LCAO — physical transparency and numerical efficiency — are maintained in this optimized scheme. It is not restricted to the muffin-tin approximation. In particular, the Hartree potential is constructed from overlapping *extended* site potentials. Hence, that part of the nonspherical effects

produced by the crystal symmetry is taken into account self-consistently. On the other hand, the intra-atomic asphericity is quenched by azimuthal averaging over the site charge density during the iterations and is only included in the final step for calculating the CF parameters.

We start with a discussion of the treatment of ionicities in our method. The assignment of a certain ionicity to atoms in a metallic compound in the framework of electronic structure calculations is rather ill-reputed. This is mainly due to the fact that the atomic site charge is frequently obtained by integrating over the charge density within a sphere and thus it is sensitive to the more or less arbitrary choice of the sphere radii. Moreover, the atomic s - and p -valence states have considerable amplitudes at the nearest neighbor positions (and beyond) and hence contribute to the charge counted as *transferred* to neighbor atoms. The charge transfer may become unphysically high if compared to what is expected from the related electronegativities. A detailed analysis of this problem can be found in Ref. 33.

Within LCAO, atomic site charges can be obtained naturally by gross population (Mulliken) analysis:

$$Q_i = -\frac{1}{\sqrt{N}} \sum_{\mathbf{kn}} \Theta(\varepsilon_F - \varepsilon_{\mathbf{kn}}) \times \sum_{lm} C_{lm,i}^*(\mathbf{kn}) e^{-i\mathbf{k}\mathbf{R}_i} \langle lm | \mathbf{k} \mathbf{n} \rangle, \quad (4)$$

where $|\mathbf{kn}\rangle$ denotes a Bloch state,

$$|\mathbf{kn}\rangle = \frac{1}{\sqrt{N}} \sum_{lm_i} C_{lm,i}(\mathbf{kn}) e^{i\mathbf{k}\mathbf{R}_i} |lm_i\rangle, \quad (5)$$

composed of atomiclike orbitals (AO's) $|lm\rangle$ at sites \mathbf{R}_i , that are orthogonal to all core states. The gross population analysis can be understood as a summation over Bloch states, projected onto atomic basis states. The main difference to conventional estimations of atomic site charges in most electronic structure calculations is that Q_i is not obtained by projecting onto an arbitrary real-space region, but onto a domain in Hilbert space. Consequently, the related site charge densities $\rho_i(\mathbf{r})$,

$$\rho_i(\mathbf{r}) = -\frac{1}{N} \sum_{\mathbf{kn}} \Theta(\varepsilon_F - \varepsilon_{\mathbf{kn}}) \sum_{l'm',i'} \sum_{lm} C_{lm,i}^*(\mathbf{kn}) C_{l'm',i'}(\mathbf{kn}) e^{-i\mathbf{k}(\mathbf{R}_i - \mathbf{R}_{i'})} \langle lm | \mathbf{r} \rangle \langle \mathbf{r} | l'm' i' \rangle, \quad (6)$$

$$\rho(\mathbf{r}) = \sum_i \rho_i(\mathbf{r}),$$

overlap, typical spatial extensions being some $6a_0$ (a_0 is the Bohr radius) in our scheme, which has to be compared to muffin-tin or Wigner-Seitz radii of typically 2–3.5 a_0 .

In this general representation, the analysis contains an equally large amount of arbitrariness as in other representations, depending on the number and shape of “atomic” (local) orbitals used. However, this arbitrariness is largely reduced in our case,³¹ where a very effective (complete) *minimum* atomic basis has been constructed. In particular, the overlap of the AO's is opti-

mized, i.e., kept as small as possible. This is achieved by adding an artificial potential V_i^{opt} ,

$$V_i^{\text{opt}}(l) = \{r/[r_{\text{WS}}^{3/2} r_{0,i}(l)]\}^4, \quad (7)$$

to the atomic site Hamiltonian H_i . Here, r_{WS} is the Wigner-Seitz radius and $r_{0,i}(l)$ are parameters used to optimize the shape of the AO's, which are eigenstates of $H_i + V_i^{\text{opt}}(l)$. The optimization is done with respect to band energies³¹ and usually yields values of $r_{0,i}(l)$ between 0.8 and 1.2.

The resulting site charges Q_i agree well with what is expected from chemical intuition, cf. our recent discussion of charge transfer in SmT_5 compounds.⁵ Obviously,

$$-\sum_i Q_i = \sum_{\mathbf{kn}} \Theta(\varepsilon_F - \varepsilon_{\mathbf{kn}}) \langle \mathbf{kn} | \mathbf{kn} \rangle = N. \quad (8)$$

This neutrality relation essentially facilitates accurate CF calculations, since the distribution of electrical monopoles is completely described by the charges Q_i . In contrast, much care is necessary in treating the interstitial charge in sphere-oriented schemes.

Different levels of accuracy are used in the calculation of the CF parameters given by Eqs. (3) and (6). The on-site terms are treated most accurately taking into account the nonspherical charge distribution ρ_0 belonging to the rare-earth site \mathbf{R}_0 . It can be subdivided into net contributions arising from terms $\langle lm0 | \mathbf{r} \rangle \langle \mathbf{r} | l'm'0 \rangle$ in Eq. (6) and overlap contributions corresponding to $\langle lm0 | \mathbf{r} \rangle \langle \mathbf{r} | l'm'i \neq 0 \rangle$. The net contributions in turn contain p - p , d - d , and s - d terms entering A_2^0 , whereas $A_4^0(\text{net})$ consists of d - d terms only. The AO's are expanded into Slater functions in our scheme, and all integrations in Eq. (3) can be done analytically for the on-site net contributions. The on-site overlap part is evaluated by direct numerical integrations (except for the inner analytical integral over the $4f$ density), where a simple cubic mesh of some 10^5 real-space points was used. We intend to improve this procedure in later applications: the overlap density could be expanded into plane waves making an analytical treatment possible.³⁴ On the other hand, only real-space integrations open the possibility of investigating the spatial origin of the crystal field, see Fig. 2.

It should be mentioned that core orthogonalization corrections to the nonspherical overlap density have been neglected. These corrections contribute 2% to the R overlap charge and influence the electric field gradient near the nucleus, but should not change the crystal field acting on the $4f$ electrons in any essential manner.

Contributions from neighbor densities overlapping with the $4f$ density, i.e., up to a neighbor distance of $10a_0$, were integrated numerically in the same way as the on-site overlap terms. Both the core electron charge Q_i^{core} and the nuclear charge Z_i contributions were added as point charges.

Concerning site charge densities not overlapping with the $4f$ charge under consideration, a spherical approximation equivalent to a PCM with point charges q_i , representing the charge transferred to atom i ,

$$q_i = Q_i + Q_i^{\text{core}} + Z_i, \quad (9)$$

was used. The number of point charges which have to be included depends on the order of the CF parameter under consideration and the corresponding cutoff radius amounts to $120a_0$, $30a_0$, and $15a_0$ for the second-, fourth-, and sixth-order parameters, respectively.

All approximations employed in the calculation of A_l^n from the charge distribution according to Eq. (3) have been checked to cause a total numerical error of less than 5%.

IV. RESULTS AND DISCUSSION

The results reported here are based on self-consistent scalar relativistic LCAO calculations similar to those described in Ref. 5. SmCo_5 crystallizes in the hexagonal CaCu_5 structure with three nonequivalent atomic sites: Sm-1(a), Co-2(c), and Co-3(g), see Fig. 1. The experimental lattice constants, $a = 9.4563a_0$ and $c = 7.5004a_0$,¹ are used. Related values for the isostructural GdCo_5 compound, which has been calculated for comparison, are $a = 9.3977a_0$ and $c = 7.5004a_0$.¹ We employed the von Barth-Hedin version for the exchange and correlation potential¹⁹ and used 152 inequivalent k points in the Brillouin-zone integrations.

The optimal values of the parameters r_0 , Eq. (7), are $r_{0,\text{Sm}}(l = 0, 2) = 1.1$; $r_{0,\text{Sm}}(l = 1) = 1.0$; $r_{0,\text{Co}}(l = 0, 2) = 0.9$; $r_{0,\text{Co}}(l = 1) = 0.8$. All results from LCAO calculations given in the tables refer to this choice. We checked the influence of changing r_0 for $i = \text{Sm}$ and for $i = \text{Co}$ separately by $\pm 5\%$ and found the following respective shift in the results: total spin moment $\pm 0.05\mu_B$, charge transfer from Sm to Co ± 0.15 , second-order CF parameter -10% , other CF parameters $\pm 10\%$.

Deviations in the local spin moments μ_s and in the charge transfer values q_i (Table I) in comparison to our earlier data on SmCo_5 (Ref. 5) result from several minor improvements in the numerical algorithm and from a different choice of the atomic basis functions (larger $r_{0,\text{Sm}}$ in the present calculation). Tables II and III contain the calculated expectation values of the radial $4f$ wave function for Sm in SmCo_5 (our calculation) and for Gd in GdCo_5 (our calculation and Refs. 9 and 17) in comparison to the free-ion Dirac-Fock results by Freeman and Desclaux.³⁵ In both cases, the bulk values are essentially larger than those calculated for the free trivalent ion, which might be attributed to the influence of the crystal potential. The mean value of the radial functions for the occupied $4f$ states is used in our calculation.

A comparison of calculated and experimental crystal-field parameters for the rare-earth site in RCO_5 is given in Table IV. Our calculated values and the experimental values for $A_2^0(r^2)$ and for A_4^0 refer to SmCo_5 , whereas the values calculated by Daalderop *et al.*^{9,17} concern GdCo_5 . In order to compare with these data, we repeated the calculation for the case of GdCo_5 and included the re-

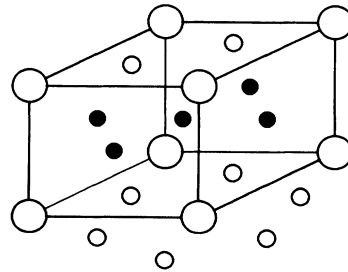


FIG. 1. The CaCu_5 crystal structure. The different atomic positions are \circ - $\text{Sm}_{1(a)}$, \bullet - $\text{Co}_{3(g)}$, \circ - $\text{Co}_{2(c)}$. The first, second, and third neighbors of Sm are 6 $\text{Co}_{2(c)}$, 12 $\text{Co}_{3(g)}$, and 2 $\text{Sm}_{1(a)}$, respectively.

TABLE I. Calculated atomic site spin moments μ_s and charge transfers q_i in SmCo_5 and in GdCo_5 . The rare-earth moment does not contain the $4f$ contribution.

Compound	Site	μ_s (μ_B)	q_i
SmCo_5	Sm 1(a)	-0.35	+0.09
	Co 3(g)	1.47	-0.03
	Co 2(c)	1.50	0.00
GdCo_5	Gd 1(a)	-0.40	+0.04
	Co 3(g)	1.46	-0.03
	Co 2(c)	1.47	+0.03

lated results in Table IV (last column). The experimental $A_6^0\langle r^6 \rangle$ value was estimated from measurements on the easy-plane compounds NdCo_5 and DyCo_5 cited in Ref. 36 by rescaling $\langle r^6 \rangle$ to that valid for Sm^{3+} (Ref. 35) and taking the mean value. In the same way we estimated $A_4^0\langle r^4 \rangle$ and $A_2^0\langle r^2 \rangle$ from data on Pr and Nd in $\text{Pr}_x\text{Nd}_{1-x}\text{Co}_5$.¹² It should be justified to compare A_7^m for different isostructural R - T compounds with the same transition metals involved, since the valence electronic structure of most rare earths (including those under consideration) is essentially the same. This assumption has recently been proven correct for the $R_2\text{Fe}_{14}\text{B}_2$ series.¹⁶ In the present calculations, a 15% difference between $A_2^0(\text{Sm})$ and $A_2^0(\text{Gd})$ is found, the differences in the higher-order parameters are negligible.

A comparison with experimental data should preferably be done for the product between the crystal-field parameter and the radial expectation value, since this product is fitted to the experimental MAE data in the semiempirical descriptions^{7,10,11,36,12} and not the individual factors. Essentially the same experimental input was used by different authors to obtain the semiempirical $A_2^0\langle r^2 \rangle$ values compiled in Table IV. In fact, Buschow *et al.*⁷ and Radwanski¹¹ refer to the same experimental data, but the former authors include the admixing of two excited Sm $4f$ multiplets, which is neglected by Radwanski. Nonetheless, both fittings yield nearly equivalent results for the second-order crystal-field parameter (however, with assumptions for the strength of the exchange field differing by a factor of 2). Sankar *et al.*¹⁰ used the same model and the same number of multiplets as Buschow *et al.*⁷ They arrive at a slightly (20%) larger exchange field, but report more than twice the value for $A_2^0\langle r^2 \rangle$. We consider this difference to be suspicious, since the fitted curves are quite similar in shape and magnitude

TABLE II. Calculated $4f$ radial expectation values $\langle r^l \rangle$ for Sm in SmCo_5 in comparison to free-ion Dirac-Fock values.

	Sm in SmCo_5 ^a	Sm^{3+} ^b
$\langle r^2 \rangle_{4f} [(a_0)^2]$	1.07	0.97
$\langle r^4 \rangle_{4f} [(a_0)^4]$	2.99	2.26
$\langle r^6 \rangle_{4f} [(a_0)^6]$	17.3	10.6

^a Present calculation.

^b Free-ion Dirac-Fock calculation (Ref. 35).

TABLE III. Calculated $4f$ radial expectation values $\langle r^l \rangle$ for Gd in GdCo_5 in comparison to free-ion Dirac-Fock values.

	Gd in GdCo_5 ^a	Gd in GdCo_5 ^b	Gd^{3+} ^c
$\langle r^2 \rangle_{4f} [(a_0)^2]$	0.94	0.93	0.87
$\langle r^4 \rangle_{4f} [(a_0)^4]$	2.32	2.11	1.82
$\langle r^6 \rangle_{4f} [(a_0)^6]$	12.2	8.58	7.83

^a Present calculation.

^b Calculation by Daalderop *et al.* (Refs. 9 and 17).

^c Free-ion Dirac-Fock calculation (Ref. 35).

to those used by the other authors. Finally, a value for the “pure” CF parameter A_2^0 is given in a recent review by Coey,²⁴ but we are not aware of the way it was determined. The fourth- and sixth-order axial parameters have been obtained from the thermal dependence of the effective spin-reorientation angle for the pseudobinary series $\text{Pr}_x\text{Nd}_{1-x}\text{Co}_5$.¹² An estimation of $A_6^0\langle r^6 \rangle$ is possible from measurements of the in-plane anisotropy of NdCo_5 and DyCo_5 , as cited in Ref. 36.

The signs of our calculated values for all CF parameters agree with the experiment. On the other hand, $A_2^0\langle r^2 \rangle$ and $A_4^0\langle r^4 \rangle$ from the calculation exceed the related semiempirical values by approximately a factor of 2–4 in magnitude. The agreement between theoretical and ex-

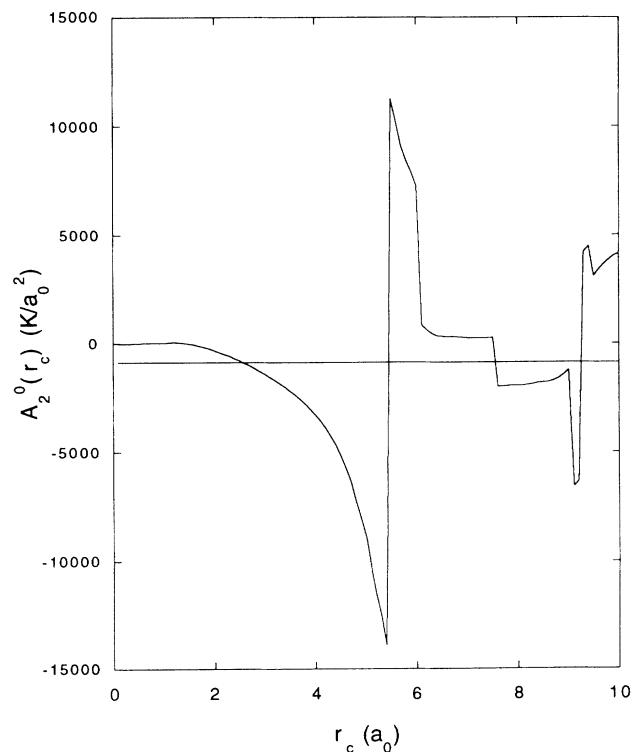


FIG. 2. Contribution to the crystal-field parameter A_2^0 for Sm in SmCo_5 from all charges within a sphere of the radius r_c . The asymptotic value $A_2^0(r_c \rightarrow \infty)$ is indicated by a straight line. Notice that core electrons of neighboring atoms are treated as point charges.

TABLE IV. Comparison of calculated and experimental crystal-field parameters $A_l^m \langle r^l \rangle$ and A_l^m for Sm in SmCo₅ (the present calculation and experimental results) and for Gd in GdCo₅ [calculations by Daalderop *et al.* (Refs. 9 and 17) and our data]. The SmCo₅ data from the present calculation are divided into on-site and lattice contributions. In addition, the on-site terms are decomposed into net (containing *p-p*, *d-d*, and *s-d*) and overlap contributions (see text); the lattice terms are separated into contributions arising from the first-, second-, third-, and fourth-neighbor atom shells and from the rest of the lattice.

	Sm in SmCo ₅			Gd in GdCo ₅		
	On site ^a	Lattice ^a	Total ^a	Experiment	Total ^b	Total ^a
$A_2^0 \langle r^2 \rangle$ [K]	-880	-50	-930	-180 ^c -420 ^d -185 ^e	-763	-950
	net: -320 <i>p-p</i> : +110 <i>d-d</i> : -410 <i>s-d</i> : -20 ovl: -560	1 +460 2 -320 3 -190 4 -17 ≥ 5 +23				
(A_2^0) [K(a ₀) ⁻²]			(-870)	(-230) ^f	(-824)	(-1010)
	Sm in SmCo ₅			Gd in GdCo ₅		
	On site ^a	Lattice ^a	Total ^a	Experiment	Total ^b	total ^a
$A_4^0 \langle r^4 \rangle$ [K]	-11	-27	-38	≈ -14 ^g	-27	-31
	net: -9 ovl: -2	1 -43 2 +26 3 -8 ≥ 4 -2				
(A_4^0) [K(a ₀) ⁻⁴]			(-13)		(-13)	(-13)
	Sm in SmCo ₅			Gd in GdCo ₅		
	On site ^a	Lattice ^a	Total ^a	Experiment	Total ^b	Total ^a
$A_6^0 \langle r^6 \rangle$ [K]	-1	+7	+6	≈ +9 ^h	+3.6	+5
		1 +9 2 -1 3 -1 ≥ 4 0				
(A_6^0) [K(a ₀) ⁻⁶]			(+0.4)		(+0.4)	(+0.4)
$A_6^6 \langle r^6 \rangle$ [K]	-20	+170	+150	≈ +230 ⁱ	+99	+100
		1 +210 2 -40 3 0 ≥ 4 0				
(A_6^6) [K(a ₀) ⁻⁶]			(+9)		(+12)	(+9)

^a Present calculation.

^b Calculation by Daalderop *et al.* (Refs. 9 and 17).

^c Reference 7.

^d Reference 10.

^e Reference 11.

^f Reference 24.

^g This value has been estimated as the mean of semiempirical values for Pr and Nd, obtained from measurements on Pr_xNd_{1-x}Co₅ (Ref. 12), rescaled with the appropriate value of $\langle r^4 \rangle$.

^h This value has been estimated as the mean of semiempirical values for Pr and Nd, obtained from measurements on Pr_xNd_{1-x}Co₅ (Ref. 12), rescaled with the appropriate value of $\langle r^6 \rangle$.

ⁱ This value has been estimated as the mean of two measurements on NdCo₅ and one result on DyCo₅, cited in Ref. 36, rescaled with the appropriate value of $\langle r^6 \rangle$.

perimental data for the sixth-order parameters seems to be better, but the $\langle r^6 \rangle_{4f}$ value is rather sensitive to details of the calculation and should be taken with some caution.

To compare with the recent FLAPW results^{9,17} on GdCo₅, the “pure” A_l^m values should be considered, which can be presumed to be virtually independent of the R atom. Here, all parameters are nearly equivalent in both calculations. Thus, from two completely independent (FLAPW and LCAO) density-functional calculations, the same — at the claimed level of accuracy — crystal-field parameters have been obtained. The 20% difference between FLAPW and LCAO results for the most sensitive parameter A_2^0 should be due to the self-consistent (non-self-consistent) treatment of the non-spherical on-site charge density in these schemes. It should be noted that the LCAO result is much closer to the FLAPW data than, e.g., a warped muffin-tin calculation¹⁷ yielding A_2^0 larger than FLAPW by a factor of 2. Thus, the continuity of the crystal potential inherent to the overlapping potential representation used in

our calculations seems to be the most essential aspect of a “full potential” treatment.

Two trends become evident from the subdivision of A_l^m into contributions arising from different parts of the charge distribution: (i) The lattice contribution is small for A_2^0 but becomes dominating with increasing order of the CF parameter. The same tendency has been found by Daalderop.¹⁷ (ii) For the quantity A_l^m (lattice), many compensating terms contribute in second order, whereas only nearest and next-nearest neighbors influence the higher orders. Specifically, the six nearest Co neighbors are responsible for creating A_6^6 , in accordance with the model suggested by Radwanski.³⁶ On the other hand, the validity of cluster calculations for the estimation of A_2^0 is disproved (compare the large contribution of the third-neighbor shell). Such calculations, in particular a *restriction* on on-site terms in a muffin-tin or Wigner-Seitz sphere,^{15,16} can give right answers only by accident. This claim is illuminated in Fig. 2, showing the contribution to A_2^0 from all charges within a sphere of the radius r_c ,

$$A_2^0(r_c) = \frac{4\pi}{5} \int_{R < r_c} d\mathbf{R} C_{20} Z_{20}(\mathbf{R}) \rho(\mathbf{R}) \int dr \frac{r_{\leq}^2}{r_{>}^3} r^2 \rho_{4f}(r) \Big/ \int dr r^4 \rho_{4f}(r), \quad A_2^0 = A_2^0(r_c \rightarrow \infty).$$

In principle, the function $A_2^0(r_c)$ should not depend on the particular charge density representation if the representation is complete enough for this purpose. The derivative $dA_2^0(r_c)/dr_c$ is quite large in the vicinity of the usual Wigner-Seitz radius, $r_c \approx 3.5a_0$, and there is no obvious reason for a *complete* cancellation of the contributions from larger distances.

Figure 3 shows, on a larger scale, the on-site contributions to $A_2^0(r_c)$. Convergency is achieved for $r_c \approx 4a_0$ and $r_c \approx 6a_0$ for the on-site net and overlap contribution, respectively. It is clearly seen that there is only a small contribution (50 K/ a_0^2) to A_2^0 from the region $r_c < 1.5a_0$, i.e., from the spatial domain of the 4f electrons. This gives *a posteriori* the justification for neglecting the exchange contributions to the crystal field.

V. CONCLUSIONS

First-principles calculations of all relevant crystal-field parameters of Sm in SmCo₅ have been carried out utilizing the “open 4f core shell” treatment. An optimized LCAO scheme has been used, involving a charge density representation highly appropriate to this task.

It has been shown that neither on-site nor lattice contributions to the CF parameters can be excluded *a priori*. Consequently, point-charge calculations taking no account of nonspherical distortions of the on-site valence charge density cannot be expected to be accurate. It might be that a cluster calculation of A_2^0 or a restriction to on-site terms can yield results of the right sign and reasonable magnitude, but this is not reliable due to the large and long-range lattice contributions. Further, the subdivision into on-site and lattice terms depends on the specific representation of the charge density. An estima-

tion of fourth- and sixth-order CF parameters by means of cluster calculations seems possible.

Within the present approach, the experimental signs of all CF parameters can be explained from a realistic

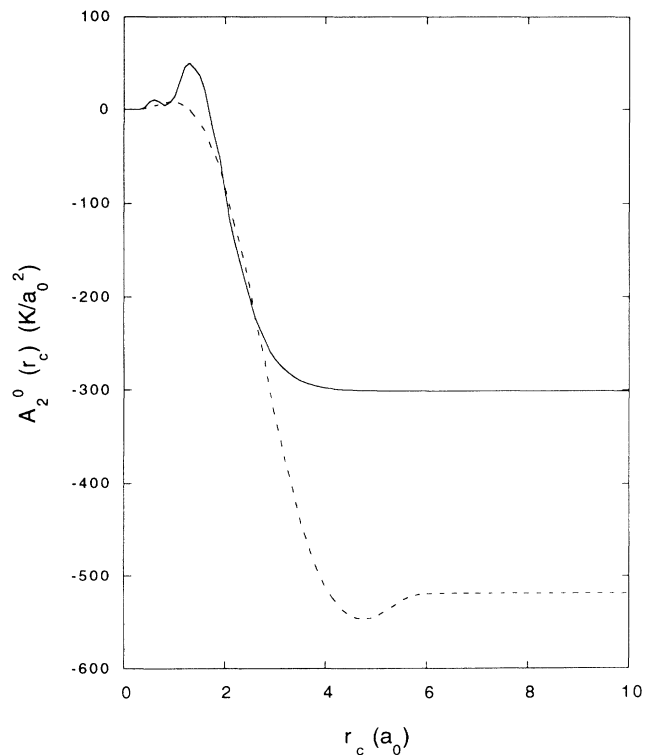


FIG. 3. Contributions to $A_2^0(r_c)$ from the on-site net charge (full line) and from the on-site overlap charge (dashed line).

ab initio charge distribution. The magnitudes of $A_2^0\langle r^2 \rangle$ and of $A_4^0\langle r^4 \rangle$, as calculated by us, exceed the related semiempirical values considerably. There is good agreement, however, between this calculation and the theoretical results by Daalderop.^{9,17} The disagreement between *ab initio* CF parameters from two independent calculations and semiempirical parameters remains an open question, which might be a challenge for improvements of the model of 4*f* magnetocrystalline anisotropy.

The following approximations have been applied and ought to be investigated in more detail: the assumed independence of A_l^m on the direction of magnetization (via the spin-orbit interaction of the valence electrons there will be such a dependence, although presumably very weak) and the exclusion of nonspherical on-site densities during the self-consistent iteration.

ACKNOWLEDGMENTS

We are indebted to M. S. S. Brooks, R. Coehoorn, J. M. D. Coey, G. H. O. Daalderop, O. Eriksson, M. Fähnle, T. Gasche, K. Hummler, J. Kübler, I. Sandalov, J. Trygg, P. Weinberger, and M. Weinert for stimulating and helpful discussions and communications. M. Aldén, S. Mirbt, L. Nordström, L. Severin, P. Söderlind, and S. Uisk contributed in many aspects to the completion of this project and made work a pleasure. Manuel Richter and Börje Johansson are grateful to the Swedish Natural Research Council for financial support, as are Peter Oppeneer and Manuel Richter to the Deutsche Forschungsgemeinschaft, SFB 252, and Helmut Eschrig to the Forschungszentrum Jülich GmbH.

*Present address: Max-Planck research group "Electron systems," Physics Dept., University of Technology, Mommsenstr. 13, D-O-8027 Dresden, Germany; electronic mail: mpag@tudurz.urz.tu-dresden.de

¹K.H.J. Buschow, Rep. Prog. Phys. **40**, 1179 (1977).

²Hong-Shuo Li and J.M.D. Coey, in *Ferromagnetic Materials*, edited by E.P. Wohlfarth and K.H.J. Buschow (North-Holland, Amsterdam, 1991), Vol. 6, p. 3.

³D. Howe, in *Supermagnets, Hard Magnetic Materials*, Vol. 331 of *NATO Advanced Study Institute, Series C: Mathematical and Physical Sciences*, edited by G.J. Long and F. Grandjean (Kluwer Academic, Dordrecht, 1991), p. 585.

⁴S.K. Malik, F.J. Arlinghaus, and W.E. Wallace, Phys. Rev. B **16**, 1242 (1977).

⁵M. Richter and H. Eschrig, Physica B **172**, 85 (1991).

⁶B. Barbara, D. Gignoux, and C. Vettier, *Lectures on Modern Magnetism* (Science Press, Beijing, 1988).

⁷K.H.J. Buschow, A.M. van Diepen, and H.W. de Wijn, Solid State Commun. **15**, 903 (1974).

⁸L. Nordström, M.S.S. Brooks, and B. Johansson, J. Phys.: Condens. Matter **4**, 3261 (1992).

⁹G.H.O. Daalderop, P.J. Kelly, and M.F.H. Schuurmans, J. Magn. Magn. Mater. **104-107**, 737 (1992).

¹⁰S.G. Sankar, V.U.S. Rao, E. Segal, and W.E. Wallace, Phys. Rev. B **11**, 435 (1975).

¹¹R.J. Radwanski, J. Magn. Magn. Mater. **62**, 120 (1986).

¹²M.R. Ibarra, L. Morella, and P.A. Algarabel, Phys. Rev. B **44**, 9368 (1991).

¹³P. Fulde, in *Handbook on the Physics and Chemistry of Rare Earth*, edited by K.A. Gschneider, Jr. and L. Eyring (North-Holland, Amsterdam, 1979), Vol. 2, p. 295.

¹⁴Xue-Fu Zhong and W.Y. Ching, Phys. Rev. B **40**, 5292 (1989).

¹⁵R. Coehoorn, in *Supermagnets, Hard Magnetic Materials* (Ref. 3), p. 133.

¹⁶K. Hummler and M. Fähnle, Phys. Rev. B **45**, 3161 (1992).

¹⁷G.H.O. Daalderop, Ph.D. thesis, Technical University, Delft, 1991.

¹⁸M.S.S. Brooks, L. Nordström, and B. Johansson, Physica

B **172**, 95 (1991).

¹⁹U. von Barth and L. Hedin, J. Phys. C **5**, 1629 (1972).

²⁰B. Johansson and A. Rosengren, Phys. Rev. B **11**, 2836 (1975); B. Johansson and P. Munck, J. Less-Common Met. **100**, 49 (1984).

²¹M.S.S. Brooks, O. Eriksson, and B. Johansson, J. Phys.: Condens. Matter **1**, 5861 (1989).

²²H. Eschrig, Physica C **159**, 545 (1989); see also H. Eschrig, in *Electronic Structure of Solids '91*, edited by P. Ziesche and H. Eschrig (Akademie-Verlag, Berlin, 1991), p. 1.

²³J. Trygg, B. Johansson, and M.S.S. Brooks, J. Magn. Magn. Mater. **104-107**, 1447 (1992).

²⁴J.M.D. Coey, in *Current Trends in the Physics of Materials*, Proceedings of the International School of Physics "Enrico Fermi", Course CVI, edited by G.F. Chiarotti, F. Fumi, and M.P. Tosi (North-Holland, Amsterdam, 1990), p. 265.

²⁵K.W.H. Stevens, Proc. Phys. Soc. A **65**, 209 (1952).

²⁶M.T. Hutchings, Solid State Phys. **16**, 227 (1964).

²⁷K.C. Das and D.K. Ray, Phys. Rev. **187**, 777 (1969).

²⁸H.H.A. Smit, R.C. Thiel, and K.H.J. Buschow, J. Phys. F **18**, 295 (1988).

²⁹A.R. Williams, J. Kübler, and C.D. Gelatt, Jr., Phys. Rev. B **19**, 6094 (1979).

³⁰H.J.F. Jansen and A.J. Freeman, Phys. Rev. B **30**, 561 (1984).

³¹H. Eschrig, *Optimized LCAO Method and the Electronic Structure of Extended Systems* (Akademie-Verlag, Berlin, 1988).

³²M. Richter, Ph.D. thesis, ZFW der AdW, Dresden, 1988.

³³R.E. Watson, M. Weinert, G.W. Fernando, and J.W. Davenport, Physica B **172**, 289 (1991).

³⁴P.M. Oppeneer, W. Hierse, and J. Kübler, Physica B **172**, 195 (1991).

³⁵A.J. Freeman and J.P. Desclaux, J. Magn. Magn. Mater. **12**, 11 (1979).

³⁶R.J. Radwanski, J. Phys. F **17**, 267 (1987).

³⁷P. Novák and J. Kuriplach, J. Magn. Magn. Mater. **104-107**, 1499 (1992).